AN ACCOUNT OF THE EFFECT OF THE PMT AFTERPULSES ON THE LIDAR SIGNALS OF AEROSOL AND MOLECULAR SCATTERING

A.V. El'nikov, V.V. Zuev, and V.N. Marichev

Institute of Atmospheric Optics,
Siberian Branch of the Academy of Sciences of the USSR, Tomsk

Received June 4, 1990

The contribution of PMT afterpulsing to the total lidar return is investigated. An attempt has been made to determine under laboratory conditions the distribution of afterpulses based on the use of the PMT impulse transfer function. The distortions due to afterpulses in lidar returns are analyzed as functions of the sensing range and pulse repetition frequency of laser in the experiments on vertical lidar sensing of the atmosphere.

INTRODUCTION

The most sensitive radiation detector in the visible and UV ranges is the photomultiplier tube (PMT). which is commonly used to detect backscattered signals in lidar systems. As any electronic device, the detector has its own shot noise. Thus in the photon counting mode an additional noise due to the so-called afterpulses (AP) occurs.[1] The afterpulses arise when the PMT is exposed to the detected light flux after the start of its action. The contribution of this effect in comparison with the illumination is small and is about 10^{-3}. However, when detecting lidar signals in the wide dynamic range, the contribution of the afterpulses becomes perceptible in comparison with the echo-signals from the far sensing ranges being 10^3–10^5 times lower than the signals from the beginning of the probing path. Therefore it becomes necessary to take into account the addition of the afterpulses in the recorded lidar signal when reconstructing the atmospheric parameters sought particularly for wide sensing ranges.

Several analytical and instrumental techniques are known, that either take into account or significantly reduce the number of afterpulses: correct account of the afterpulses with their subsequent subtraction from the detected signal, optical, shielding, and electronic strobing the PMT.[2,3,4] Their use in every specific case requires a corresponding experimental and methodological study.

The present article analyzes the possibility of using two well-known techniques for reducing the effect of afterpulsing by considering a high–altitude lidar[5] along with the experimental results of investigation of the afterpulses themselves and their effect, e.q., on the reconstructed value of the lidar scattering ratio

$$R(H) = 1 + \beta_\pi^a(H)/\beta_\pi^m(H) \qquad (1)$$

where β_π^a is the aerosol backscattering coefficient and β_π^m is the molecular backscattering coefficient. In addition a technique is described of estimating the afterpulses retrieved from lidar data on the basis of assumption that there is no aerosol in a certain section of the sensing path with the help of corresponding regression formulas.

I. ACCOUNT OF AFTERPULSING ON THE BASIS OF THE PMT IMPULSE TRANSFER CHARACTERISTIC

A simple enough and effective technique of taking into account the afterpulses described in Ref. 3 is of interest for us. The echo-signal corrected for afterpulsing of a single strobe is determined according to the formula

$$X(K) = Y(K) - \sum_{M=0}^{K-1} H(K-M)\, Y(M)\,, \; K = 1, 2, \ldots, N, \quad (2)$$

where N is the number of time Intervals (strobes), $X(K)$ is the echo–signal corrected for the afterpulsing, $Y(K)$ is the recorded echo–signal, $H(K - M)$ is the impulse transfer characteristic (ITC) of the PMT.

The ITC is the experimentally determined function normalized by a single recorded counting. It is specified for concrete model of the PMT. Measurements of this characteristic for the FÈU–130 photomultiplier used in our lidar[5] were carried out in the following way. The photon counter was triggered, then, with a certain time delay, the laser was started up. The laser beam fell on the diffusely scattering screen, and through a diaphragm of a variable diameter (to obtain various levels of the PMT illumination) passed to the lidar receiving system, and then to the PMT.

The experimentally retrieved ITC's for the illumination pulses of duration 200 ns (duration of laser pulses) with repetition frequency 2.6 – 36 MHz are shown in Fig. 1. It-was found that the impulse transfer characteristic of one and the same PMT differ strongly depending on the illumination. In this study the following effect was established: as repetition frequency of the illumination pulses increase the time of occurrence of the afterpulses becomes greater and the total number of afterpulses increases along with the number of afterpulses during the selected time intervals. The dependence of the total number of afterpulses on the repetition frequency of illumination pulses is presented in Fig. 1*b*. The resulting functional dependence obtained with the help of the regression analysis of the available experimental points has the form

$$N_{AP} = 0.002 \cdot e^{0.08 \cdot I} \qquad (3)$$

0235-6880/91/02 175–6 $02.00

where N_{AP} is the repetition frequency of afterpulses, in MHz, and I is the the repetition frequency of illumination pulses, in MHz.

It is obvious, that the existing dependence of the number of afterpulses on the the repetition frequency of illumination pulses significantly complicates the problem of correct account of afterpulsing.

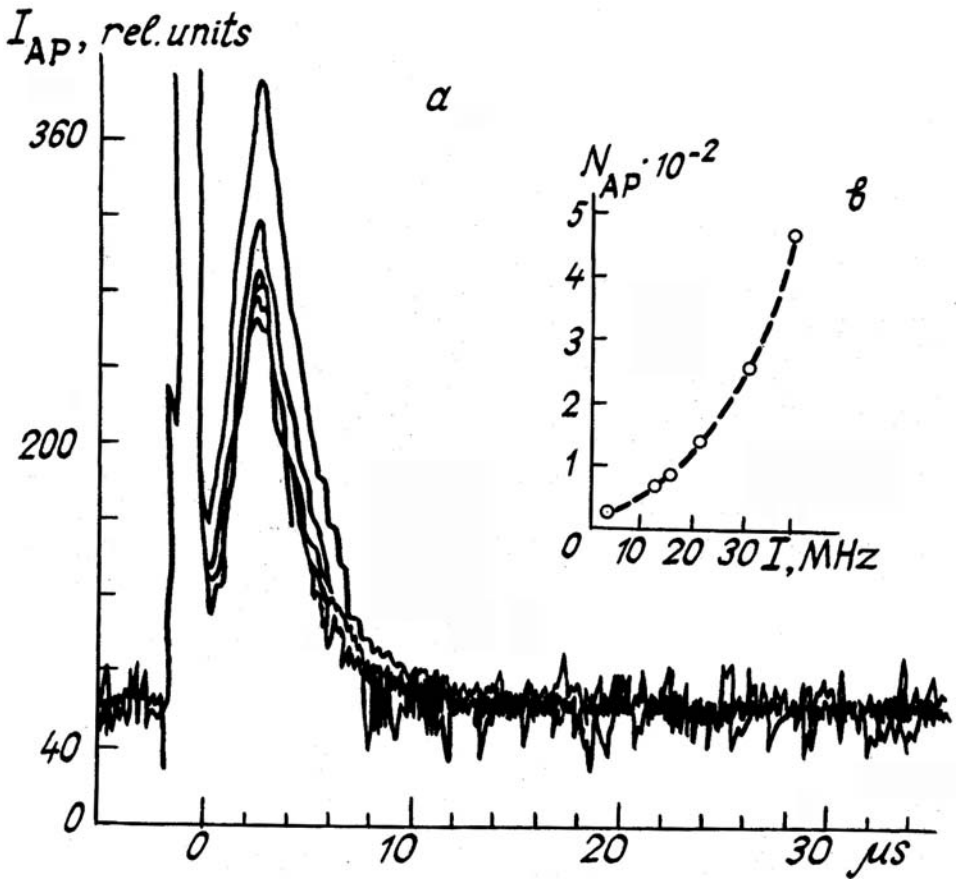

FIG. 1. Determination of the impulse trasfer characteristics of PMT from illumination by laser pulse: the temporal distribution of the repetition frequency of afterpulses (a) and the total number of afterpulses as a function of the repetition frequency of the illumination pulses (b).

In addition, one can see that the ITC is significant only within a limited time interval of 20 μs. The ITC's described elsewhere,[5,6] are also temporally limited (6 μs according to Ref. 5 and 12 μs according to Ref. 6). If this is the case, the afterpulses from the near zone of lidar (with impulse illumination) must in no way affect the far section of the probing path, because these two sections are timely separated by much more than 20 μs. However, our measurements[5] of the vertical aerosol profile with the help of the lidar, which we performed since 1986 indicated the presence of the excess signal pulses due to afterpulsing of the end of the probing path. Below we present some experimental evidence of this conclusion.

Such a discrepancy may be interpreted in such a way that an account and the correction of the signals for afterpulsing with the help of formula (2) inadequately describes the actual mechanism of afterpulsing in the PMT. This formula may be employed certainly for limited time intervals, where the ITC is defined. However, the feasibility of such a procedure for every given lidar must be considered separately. For example, for the lidar described in Ref. 5 the maximum repetition rate of afterpulses is less than 10 MHz. According to formula (3), this results in occurrence of such a number of afterpulses which is less than 0.57. of the signal pulses themselves.

OPTICAL SHIELDING OF THE PMT

Since it is impossible to correctly take into account the afterpulses with the help of the above technique, We decided to employ the optical-shielding of the PMT. The instrumental development of this problem has resulted in fabrication of electromechanical shutter, whose functional part playing the role of shielding was designed as a sector disk. The opaque sectors of this disk covered the field of view of the PMT at the moment in which the radiation from the near section of the probing path arived. Thus the starting pulse of laser could be delayed at a time determined by the sizes of the blind zone. The shutter provided for the variation of the blind zone within the 0–24 km range, while the laser was started up at a frequency varying from zero to 1.1 kHz. There exist a possibility to reverse the operating mode, i.e., to receive the signal from the hear zone and to cover the signal from the far zone.

Using the shutter in the reverse mode enables us to observe afterpulsing which distort the lidar signal at the

end of the probing path. Figure 2 shows the signal recorded for two different atmospheric situations: Fig. 2, a was obtained under conditions of continuous clouds below 4 km and Fig. 2*b* was obtained for rather clear atmosphere with thin Cirrus within the 8 – 9 km altitude range. For clear representation both profiles are divided into two parts. The first part (I) includes the near zone of the probing path and the section in which the field of view of the lidar is covered by the vane of the disk and the second part (II) includes the section of complete covering of the field of view of the lidar. The decaying signal observed at an altitude of 17 km and higher in Fig. 2*a* and at an altitude of 20 km and higher in Fig. 2*b* represents the afterpulses due to intense illuminance from the near zone. Their number gradually decreases, but at the end of the path they are still noticeable and their values significantly exceed the PMT dark current. Taking into account the decay of the desired signal which is proportional to $\beta_\pi(H)/H^2$ we found that their contribution to the received signal significantly increases. This results in an erroneous increase of the reconstructed parameter R with increase of an altitude H.

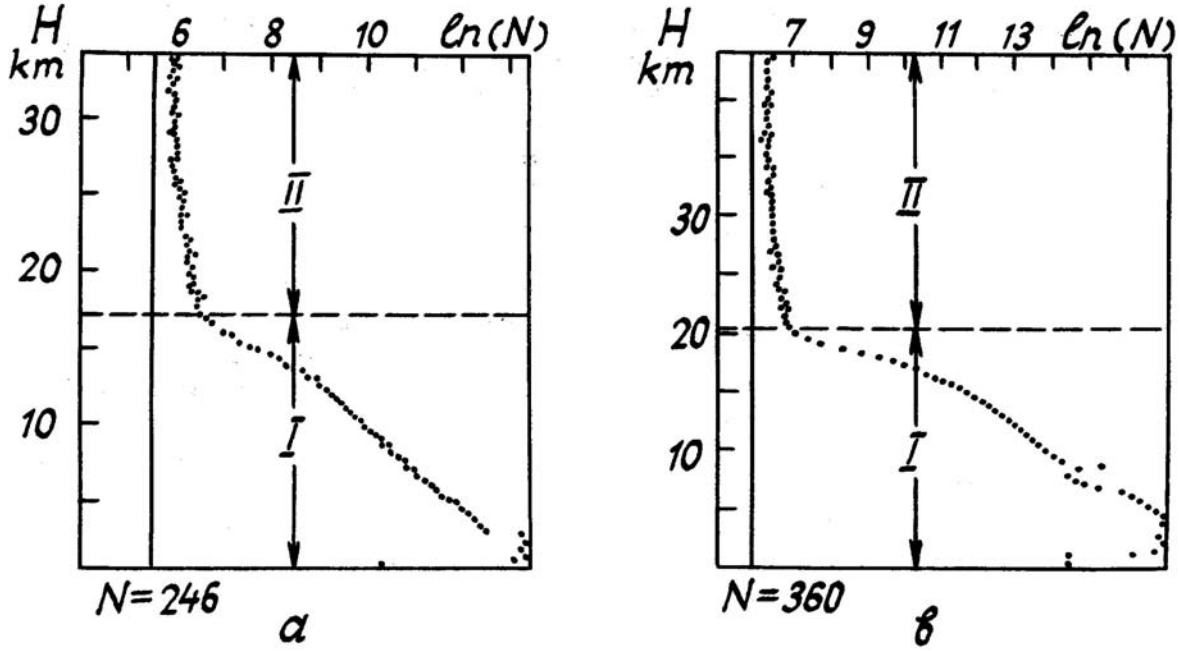

FIG. 2. Manifestation of afterpulsing in lidar returns from continuous cloud cover (a) and clear atmosphere(b).

Our seeking for universal empirical dependence of the number of the afterpulses on the received signal was unsuccessful because of the fact that this dependence is, most likely, a complicated function of a number of parameters determined by the PMT operational mode, the energetics of the laser, and the atmospheric situation. Therefore, to determine it, more careful experiments are needed. Nonetheless, we established that the number of the afterpulses in the section of the path, where they significantly distort the signal, may be represented as a sum of two terms: a constant N_0 and a variable component $\tilde{N}(H)$ decreasing with increase of height H. The ratio $\tilde{N}(H)/N_0$ remains unchanged from measurement to measurement. This allowed us to derive from the available independent data within the 16 – 40 km altitude range the following dependence:

$$\frac{\tilde{N}(H)}{N_0} = 4.7 \exp(-0.13\,H).$$

The formula for the total number of afterpulses $N(H)$ acquires the form

$$N_{AP}(H) = N_0\,[1 + 4.7 \cdot \exp(-0.13 \cdot H)]. \qquad (3)$$

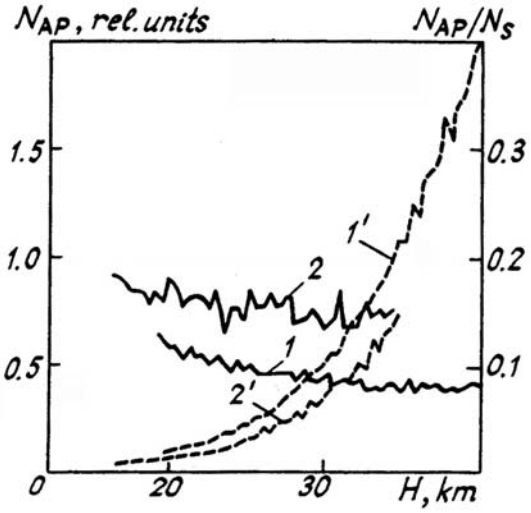

FIG. 3. Distribution of afterpulsing contribution along the vertical sensing path: the afterpulses (1 and 2) and those corrected for the backscattering coefficient and squared distance (1′ and 2′).

Further experimental studies of the afterpulses at various modes of lasing made it possible to recognize their dependence on the pulse repetition frequency of laser (Fig. 4). This dependence manifests itself in an erroneous increase of the scattering ratio $R(H)$ at altitudes above 20 km. Thus, for a frequency of 3 kHz (Fig. 4*a*) the afterpulses begin to appear from a height of approximately 20 km, and their contribution to the actual echo–signal grows with height in analogy with the case of Fig. 3. This erroneous increase in R is observed from an altitude of approximately 27 km at a pulse repetition frequency of 2 kHz (Fig. 4*b*), and the value of R at the tail–end of the probing path is much less than in the previous case. As to sensing at a frequency of 1 kHz (Fig. 4*c* and *d*), the vertical profile of the scattering ratio R becomes much closer to the actual one than in the previous cases shown in Figs. 4*a* and *b*). Therefore, the number of afterpulses may be substantially decreased by increasing the period of lasing of laser pulses (by decreasing the pulse repetition frequency).

The identical behavior of the scattering ratio R due to the presence of afterpulsing at a pulse repetition frequency of 1 kHz in the cases in which there is a cutoff of the near zone (Fig. 4*d*) and there is no cutoff (Fig. 4*c*) with increase of R to approximately 1.2 at altitudes above 30 km is observed not always. More often the use of the electromechanical shutter reduces the afterpulses to such a level that their contribution to the echo-signal at the far end of the probing path becomes negligible. This is essentially true when the zone covering exceeds 10 km.

However, the application of the given technique for PMT shielding is not so effective in the case of a lidar with high pulse repetition frequency, because the sensing range is reduced, while limiting the pulse repetition frequency by 1 kHz increases the integrating time for obtaining a statistically reliable profile. The potentialities of a lidar are artificially reduced, which is particularly inefficient for a lidar intended for regular observations. Therefore, it would be more reasonable to neutralize the effect of afterpulsing in processing of lidar signals.

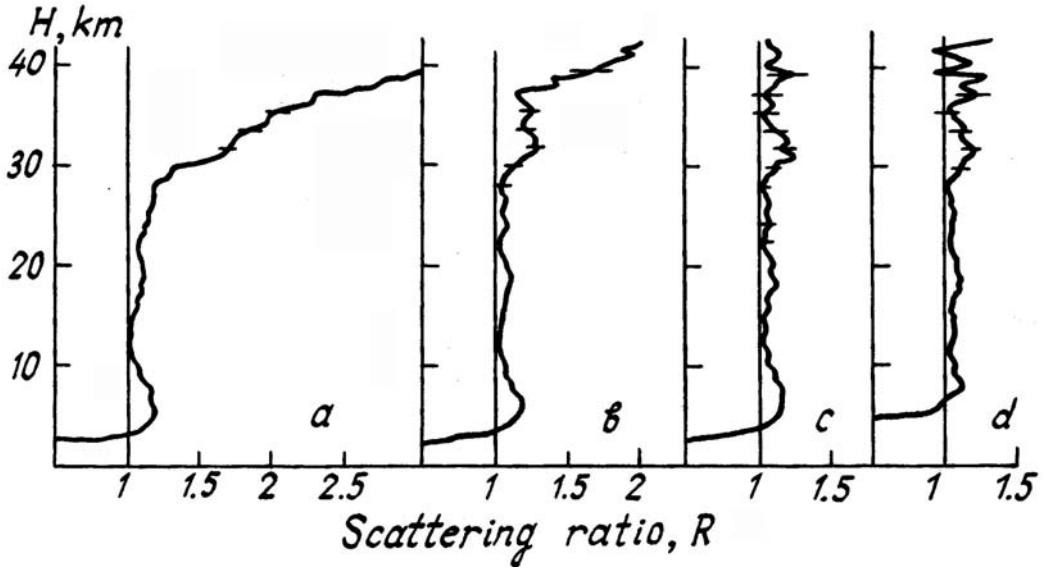

FIG. 4. Effect of afterpulsing on retrieval of the scattering ratio profile at frequencies of 3 kHz *(a),* 2 kHz *(b),* 1 kHz*(c), and* 1 kHz *with signal cutoff from the near zone using the shutter (d).*

RETRIEVAL OF THE SCATTERING RATIO FROM THE CALIBRATION SECTION OF THE PATH

It can be seen from the above results that the equation of remote sensing must be written in the form

$$N(H)=\frac{C\beta_\pi(H)T^2(H)}{H^2}+N_{BG}+N_{\mathrm{AP}}(H), \qquad (4)$$

where H is the altitude, $N(H)$ is the recorded echo–signal, C is the instrument constant, $\beta_\pi(H)$ is the total backseattering coefficient, $T(H)$ is the atmospheric transparency, N_{BG} is the background signal, and $N_{\mathrm{AP}}(H)$ are the afterpulses. Below, to simplify Eq. (4) we omit the term N_{BG} because its value can be found from the field observations.

Dividing Eq. (4) by the molecular backscattering coefficient $\beta_\pi^{\mathrm{m}}(H)$, found from the meteorological data[5], and representing $T(H)$ via its molecular T_{m} and aerosol T_{a} components

$$T_{\mathrm{m}}(H)=\left[-\frac{1}{g_{\mathrm{m}}}\int_0^H\beta_\pi^{\mathrm{m}}(z)dz\right],$$

where g_{m} is the lidar molecular ratio, and

$$T_{\mathrm{a}}(H)=\exp\left[-\int_0^{h^*}\alpha_{\mathrm{a}}(z)dz\right]\cdot\exp\left[-\int_{h^*}^{H}\alpha_{\mathrm{a}}(z)dz\right],$$

where α_{a} is the total aerosol scattering coefficient, we can write Eq. (4) in the form

$$\frac{N(H)\cdot H^2}{\beta_\pi^{\mathrm{m}}\cdot T_{\mathrm{m}}^2(H)}=C\cdot\exp\left[-2\int_0^{h^*}\alpha_{\mathrm{a}}(z)dz\right]\cdot\exp\left[-2\int_{h^*}^{H}\alpha_{\mathrm{a}}(z)dz\right]\cdot R(H)+$$

$$+\frac{N_0\,[1+4.7\cdot\exp(-0.13\cdot H)]\cdot H^2}{\beta_\pi^{\mathrm{m}}\cdot T_{\mathrm{m}}^2(H)} \qquad (5)$$

The point h^* is selected at an altitude in which the contribution of the total aerosol scattering coefficient to the atmospheric transparency becomes negligible with further ncrease of the altitude

$$\exp\left[-2\int_{h^*}^{H}-\alpha_{\mathrm{a}}(z)dz\right]=1.$$

Such an equality is satisfied fairly well at altitudes $h^* > 25$ km. The reasoning here is that under typical conditions the relative contribution of aerosol to stratospheric air transparency turned out to be much smaller than the molecular one not only for the natural aerosol but also for the aerosol which penetrates from the troposphere at altitudes $H > 25$ km and with further increase of the altitude the aerosol contribution becomes even smaller.[7,8] In vertical laser sensing the contribution of aerosol scattering to the total backscattering in the visible range is still smaller because of the smaller value of the scattering phase function. Therefore one may assume with a high degree of confidence that $R(H) \approx 1$ at $h^* > 30$ km.

On the account of these assumptions, formula (5) may be written as

$$S(H) = C_0 + N_0F(H), \text{ when } h^* \le H \le H_{\max}, \qquad (6)$$

where

$$S(H)=\frac{N(H)\cdot H^2}{\beta_\pi^{\mathrm{m}}\cdot T_{\mathrm{m}}^2(H)}, \qquad (7)$$

$$C_0 = C\cdot\exp\left(-2\int_0^{h^*}\alpha_{\mathrm{a}}(z)\mathrm{d}z\right), \qquad (8)$$

$$F(H)=\frac{[1+4.7\cdot\exp(-0.13\cdot H)]\cdot H^2}{\beta_\pi^{\mathrm{m}}\cdot T_{\mathrm{m}}^2(H)}, \qquad (9)$$

and $H_{\max}$ is the maximum altitude at which the signal is recorded with high enough accuracy.

The unknown constants C_0 and N_0 in the given formula are linearly interdependent. Hence, using the regression analysis technique they can be determined, according to Refs. 9 and 10, as

$$N_0=\frac{\sum_{\mathrm{i}=1}^{\mathrm{k}}(F(H)-\overline{F})\cdot(S(H)-\overline{S})}{\sum_{\mathrm{i}=1}^{\mathrm{k}}(F(H)-\overline{F})} \quad \text{and} \quad C_0=\overline{S}-N\overline{F}. \qquad (10)$$

Here κ is the number of strobes in the interval $(h^* - H_{\max})$, $\overline{S}$, and $\overline{F}$ are the average values of the corresponding variables in the indicated interval.

The accuracy of determination of these constants may be expressed via the standard deviation (δ^2) of $S(H)$ and $F(H)$ from the specified straight line of the form

$$\delta^2=\frac{\sum_{\mathrm{i}=1}^{\mathrm{k}}(S(H)-\overline{S})^2-N_0^2\sum_{\mathrm{i}=1}^{\mathrm{k}}(F(H)-F)^2}{(k-2)} \qquad (11)$$

as

$$(\delta N_0)^2=\frac{\delta^2}{\sum_{\mathrm{i}=1}^{\mathrm{k}}(F(H)-F)^2},$$

and

$$(\delta C_0)^2=\delta^2\left\{\frac{1}{2}+\frac{F^2}{\sum_{\mathrm{i}=1}^{\mathrm{k}}(F(H)-\overline{F})^2}\right\}^{-1}. \qquad (12)$$

Returning back to formula (5) and grouping its terms in an appropriate way we derive

$$R(H)\exp\left(-2\int_{h^*}^{\mathrm{H}}\alpha_{\mathrm{a}}(z)\mathrm{d}z\right)=\frac{\{N(H)-N_0F(H)\}\cdot H^2}{C_0\beta_\pi^{\mathrm{m}}(H)\cdot T_{\mathrm{m}}^2(H)}\equiv B(H), \qquad (13)$$

Finally, expression (13) is reduced to the equation

$$T_{\mathrm{a}}^2(h^*,H)-\frac{g_{\mathrm{a}}(H)}{2\beta_\pi^{\mathrm{m}}(H)}-\frac{\mathrm{d}T_{\mathrm{a}}^2(h^*,H)}{\mathrm{d}H}=B(H), \qquad (14)$$

where $g_a(H)$ is the lidar aerosol ratio. The solution of this equation has been considered in detail in Ref. 11, and $R(H)$ can be written as

$$R(H)=\frac{B(H)}{T_{\mathrm{a}}^2(h^*,H)}. \qquad (15)$$

According to Ref. 12, the rms error of retrieval of $R(H)$ given that covariances between the variables that determine R are small has the form

$$[\delta R(H)]^2=\left(\frac{\partial R(H)}{\partial N}\right)^2[\delta N]^2+\left(\frac{\partial R(H)}{\partial N_0}\right)^2[\partial N_0]^2+\left(\frac{\partial R}{\partial C_0}\right)^2[\delta C_0]^2, \qquad (16)$$

where $[\delta N]^2$ is the rms error in determining $N(H)$, which is equal to the quantity $N(H)$ for the Poisson point process $[\delta N_0]^2$ and $[\delta C_0]^2$ are the rms errors in calculating N_0 and C_0 defined according to Eq. (6).

In this case the relative error in determining $R(H)$ is equal to

$$\frac{\delta R(H)}{R(H)} = \sqrt{\frac{N(H)}{[N(H) - N_0 F(H)]^2} + \frac{(\delta N_0)^2 \cdot F(H)}{[N(H) - N_0 F(H)]^2} + \frac{(\delta C_0)^2}{C_0^2}}. \quad (17)$$

The profiles computed from the routine experimental data following the standard technique[5] and the indicated technique are presented in Fig. 5. It can be seen that the additional term $N_{AP}(H)$ which enters Eq. (4) and which we ignore in the standard technique results in significant distortion of the profile at altitudes in which it becomes comparable to $N(H)$.

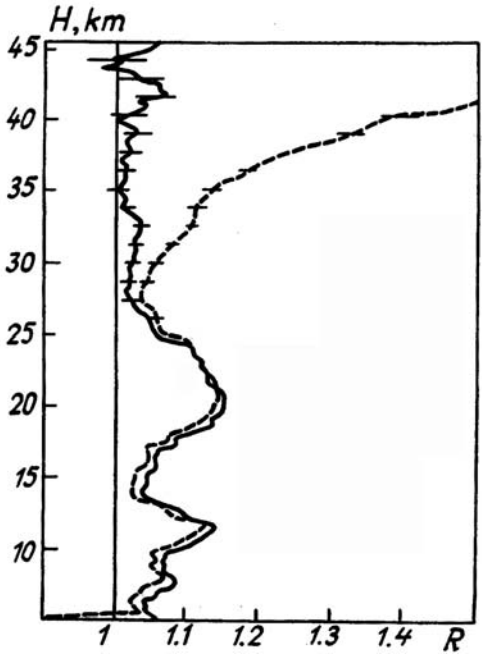

FIG. 5. Retrieval of the scattering ratio according to the procedures with account of afterpulsing (solid curve) and without it (dashed curve).

In conclusion of this section it should be noted that sufficiently small values of the ratios $\tilde{N}(H)/N_0$ for the far zone and $N_{AP}(H)/N(H)$ for the near zone permit one to neglect the variable part and to obtain a profile analogous to that shown by the solid line in Fig. 5. The parameter N_0 can be found by the trial–and–error method following the reasoning given above. It is this approach which was used in processing the experimental data obtained with the help of our lidar[5] to retrieve the scattering ratio.

CONCLUSION

The present article describes a technique of taking into account afterpulsing based on the PMT impulse transfer characteristic. An attempt to use it is made in sensing the midstratospheric vertical profile of the aerosol. It is demonstrated from the field data that there are afterpulses in lidar echo-signals that affect the retrieval of the scattering ratio $R(H)$. The dependence of the number of afterpulses on the pulse repetition frequency of laser has been experimentally discovered. The regression technique of data calibration using a section of the probing path has been described.

REFERENCES

1. S.S. Vetokhin, I.R. Gulakov, A.N. Pertsev, et al., *Single–Electron Photodetectors* (Energoatomizdat, Moscow, 1986), 160 pp.
2. A.I. Abramochkin, P.M. Holle, and A.A. Tikhomirov, in: *Measuring Devices for Studying the Parameter of Atmospheric Surface Layers,* Tomsk Affiliate of the Siberian Branch of the Academy of Sciences of the USSR, Tomsk, (1977), pp. 152–156.
3. Yu.F. Arshinov, S.M. Bobrovnikov, A.I. Nadeev and K.D. Shelevoi, in: *Abstracts of Papers Presented at the 8th All–Union Symposium on Laser and Acoustic Sounding of the Atmosphere,* Tomsk (1984), Vol. 2, pp. 280–282.
4. Y. Iikura, N. Sugimoto, Y. Sasano, and H. Shimzu, Appl. Opt. **26**. No. 24, 5299–5306 (1987).
5. A.V. El'nlkov, V.N. Marichev, and K.D. Shelevol, Opt. Atm. **1**, No. 4, 117–123 (1988).
6. D.V. Stoyanov, A.K. Donchev, G.V. Kolarov, and Ts.A. Mitsel", Opt. Atm. **1**, No. 4, 109–116 (1988).
7. V.E. Zuev and G.M. Krekov. *Optical Models of the Atmosphere* (Gidrometeoizdat, Leningrad, 1986), 256 pp.
8. M.L. Asaturov, M.I. Bud'ко, K.Ya. Vinnikov, et al., *Volcanoes, Stratospheric Aerosol, and Climate of the Earth* (Gidrometedizdat, Leningrad, 1986), 256 pp.
9. V.P. D'akonov, *Guide on Algorithms and Programs In BASIC for Personal Computers* (Nauka, Moscow, 1987), 239 pp.
10. V.K. Grishin, F.A. Zhivopistsev, and V.A. Ivanov, *Mathematical Treatment and Interpretation of Physical Experiment* (Moscow State University, Moscow, 1988), 387 pp.
11. A.V. El'nikov, S.I. Kavkyanov, G.M. Krekov, and V.N. Marichev, Atm. Opt. **2**, No. 5, 438–440 (1989).
12. R. Mezheris, *Laser Remote Sensing* [Russian Translation) (Mir, Moscow, 1987), 550 pp.